JCI insight

RESEARCH ARTICLE

MicroRNA-125a and -b inhibit A20 and MAVS to promote inflammation and impair antiviral response in COPD

Alan C-Y. Hsu,[1] Kamal Dua,[1] Malcolm R. Starkey,[1] Tatt-Jhong Haw,[1] Prema M. Nair,[1] Kristy Nichol,[1] Nathan Zammit,[2] Shane T. Grey,[2] Katherine J. Baines,[1] Paul S. Foster,[1] Philip M. Hansbro,[1] and Peter A. Wark[1,3]

[1]Priority Research Centre for Healthy Lungs, Hunter Medical Research Institute and The University of Newcastle, New South Wales, Australia. [2]Transplantation Immunology Group, Immunology Division, Garvan Institute of Medical Research, Sydney, New South Wales, Australia. [3]Department of Respiratory and Sleep Medicine, John Hunter Hospital, Newcastle, New South Wales, Australia.

Influenza A virus (IAV) infections lead to severe inflammation in the airways. Patients with chronic obstructive pulmonary disease (COPD) characteristically have exaggerated airway inflammation and are more susceptible to infections with severe symptoms and increased mortality. The mechanisms that control inflammation during IAV infection and the mechanisms of immune dysregulation in COPD are unclear. We found that IAV infections lead to increased inflammatory and antiviral responses in primary bronchial epithelial cells (pBECs) from healthy nonsmoking and smoking subjects. In pBECs from COPD patients, infections resulted in exaggerated inflammatory but deficient antiviral responses. A20 is an important negative regulator of NF-κB–mediated inflammatory but not antiviral responses, and A20 expression was reduced in COPD. IAV infection increased the expression of miR-125a or -b, which directly reduced the expression of A20 and mitochondrial antiviral signaling (MAVS), and caused exaggerated inflammation and impaired antiviral responses. These events were replicated in vivo in a mouse model of experimental COPD. Thus, miR-125a or -b and A20 may be targeted therapeutically to inhibit excessive inflammatory responses and enhance antiviral immunity in IAV infections and in COPD.

Introduction

Influenza A viruses (IAVs) are among the most important infectious human pathogens that cause enormous morbidity and mortality worldwide. This largely results from seasonal influenza, but an important feature of the biology of IAVs is the frequent emergence of novel pandemic strains/subtypes. Infections cause symptoms ranging from mild to severe viral pneumonia, with uncontrolled inflammation in the airways.

Bronchial epithelial cells (BECs) are the primary site of IAV infection, and innate immune responses produced by these cells are important in the early protection against the viruses (1, 2). During infection, viral RNAs are recognized by TLR3 and retinoic acid-inducible gene-I (RIG-I). Upon binding of TLR3 to viral RNAs, signalling pathways are initiated that activate receptor interacting protein 1 (RIP1) by ubiquitination. Activated RIP1 indirectly phosphorylates IκBα, leading to the release of active p65 and p50 subunits of NF-κB into the nucleus, where they induce the transcription of inflammatory genes including cytokines such as IL-6, TNF-α, and IL-1β and chemokines such as CXC chemokine ligand-8 (CXCL-8/IL-8) (3–5). These inflammatory cytokines recruit immune cells, in particular macrophages and neutrophils, to the site of infection that phagocytose pathogens and apoptotic cells (6, 7). RIG-I interacts with mitochondrial antiviral-signaling protein (MAVS), which activates interferon regulatory factor 3 (IRF3) by phosphorylation. Activated IRF3 then translocates into the nucleus, where it initiates the production of type I and III IFNs (8, 9). These innate cytokines induce the transcription of over 300 IFN-stimulated genes (ISGs), including the Mx1 protein that disrupts virus replication (10).

The control of inflammation is critical to achieving optimal inflammatory responses that clear viruses without excessive damage to host tissues and airways. We have previously shown that A20, also known as TNF-α–inducing protein 3 (TNFAIP3), is a negative regulator of NF-κB–mediated inflammation that

Authorship note: PMH and PAW are co–senior authors.

Conflict of interest: The authors have declared that no conflict of interest exists.

Submitted: October 24, 2016
Accepted: February 9, 2017
Published: April 6, 2017

Reference information:
JCI Insight. 2017;2(7):e90443. https://doi.org/10.1172/jci.insight.90443.

functions by targeting RIP1 for degradation, and therefore suppresses NF-κB activation (11–14). MicroRNAs (miRNAs) are another important class of immune signaling regulators that silence gene expression by degradation (15). miR-125a and -b have recently been shown to directly inhibit A20, leading to increased NF-κB activation (16). It is currently unknown if A20 or miR-125a or -b regulates type I and III IFNs during IAV infections.

Chronic obstructive pulmonary disease (COPD) is the third leading cause of illness and death globally and is characterized by progressive airway inflammation, emphysema, and reduced lung function (17). The most important risk factor for COPD in Western societies is cigarette smoking (18). COPD patients have increased susceptibility to IAV infections that cause acute exacerbations and result in more severe symptoms, disease progression, and increased mortality (19–21). Current therapeutics remain limited to vaccination and antiviral drugs. These have major issues with the constant need for developing new vaccines. COPD patients respond poorly to vaccination, as IAVs have become drug resistant and all therapeutics have questions surrounding availability and efficacy in future pandmics (22, 23). There is therefore an urgent need to develop novel therapeutics for influenza, especially for those most susceptible to infection.

Despite inflammatory signalling pathways being well characterized, the mechanisms underlying the exaggerated inflammatory responses to IAV, including in COPD, are unclear. It is known that increased NF-κB activation is elevated in biopsies from COPD patients (24). We have previously shown that human influenza H3N2 infection induced heightened inflammatory responses (25), and high pathogenic avian H5N1is known to induce severe cytokine storms in the lung (9, 26). We also showed that primary BECs (pBECs) from COPD subjects and our established in vivo model of experimental COPD have increased inflammatory and impaired antiviral responses to IAV infections, leading to more severe infection (27–29). Furthermore, miRNAs are known to be altered in COPD (30, 31). However, the molecular mechanisms underpinning the heightened inflammatory response in IAV infections and defective immune responses in COPD remain unclear. In this study, we investigated the mechanisms involved using our established experimental systems (27, 32–34). We found that COPD pBECs and mice with experimental COPD infected with IAV have higher levels of inflammatory cytokines but reduced antiviral responses (30, 35). We uncovered that NF-κB–mediated inflammation in IAV infection and in COPD was also exaggerated and resulted from decreased levels of A20 protein, which in turn was caused by elevated levels of miR-125a or -b. Treatment with specific antagomirs against miR-125a or -b reduced NF-κB activation but also increased type I and III IFN production and suppressed infection. We then found that miR-125a and -b directly target MAVS 3′-UTR, thereby suppressing the induction of type I and III IFNs. This study therefore discovers an miR-125–mediated pathway that reduces A20 and MAVS, promotes excessive inflammation, and increases susceptibility to IAV infection in COPD. It also identifies potential therapeutic options that reduce IAV-mediated inflammation and reverse immune signaling abnormalities in COPD.

Some of the data has been previously reported in abstract form (36).

Results

IAV infection induces increased inflammatory but reduced antiviral responses ex vivo in human COPD pBECs. pBECs from healthy nonsmoking control subjects, COPD patients (ex-smoker), or smoking (smoker) controls were infected with IAV H3N2 or H1N1 (MOI 5). Virus replication was measured 24 hours after infection. Virus titers increased at 24 hours (Figure 1A) and were 2-fold greater in COPD pBECs compared with controls. Infection resulted in the production of the proinflammatory cytokines/chemokines IL-6, CXCL-8, TNF-α, and IL-1β and antiviral cytokines type I (IFN-β) and type III interferons (IFN-λ1) (Figure 1B). In COPD, the induction levels of cytokines were substantially higher (2.5–10 fold) compared with healthy control and smoker pBECs (Figure 1B). In contrast, the induction of IFN-β and IFN-λ1 proteins were reduced in COPD.

We then measured the levels of activity of NF-κB by assessing the levels of phosphorylated p65 (phospho-p65) at Ser536 (35, 37, 38). Infection significantly increased the activation of phospho-p65 in both healthy and smoker pBECs at 6 hours, which was further increased at 24 hours (Figure 1C and Supplemental Figure 1A; supplemental material available online with this article; https://doi.org/10.1172/jci.insight.90443DS1). In COPD pBECs, the protein levels of phospho-p65 was elevated at baseline (media controls) at 6 hours and significantly increased with infection at 24 hours compared with healthy and smoker controls.

IAV infection also induces increased inflammatory but reduced antiviral responses in vivo in experimental COPD. We then demonstrated these events also occur in vivo. BALB/c mice were exposed to either normal air (Air) or cigarette smoke (Smk) for 8 weeks. The Smk group develops hallmark features of

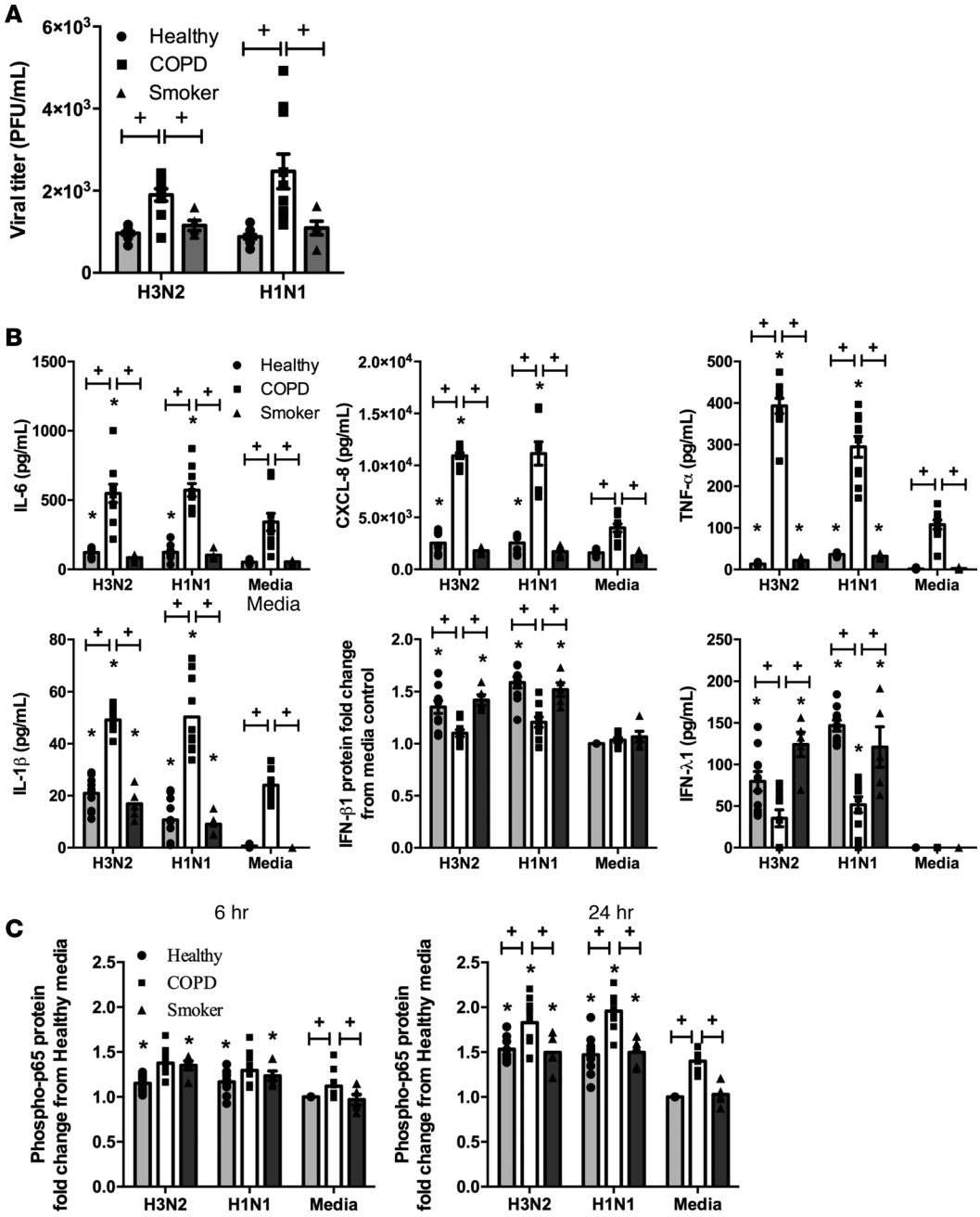

Figure 1. IAV infection is more severe and results in exaggerated inflammatory but impaired antiviral responses in pBECs from patients with COPD. pBECs from healthy controls, COPD patients, and healthy smokers were infected with human IAV H3N2 or H1N1, and (**A**) virus replication was measured at 24 hours. (**B**) Proinflammatory cytokines/chemokines IL-6, CXCL-8, TNF-α, and IL-1β and antiviral cytokines IFN-β and IFN-λ1 were measured in culture supernatants at 24 hours. (**C**) Phospho-p65 was assessed at 6 hours and 24 hours, and densitometry results (from Supplemental Figure 1A, representative immunoblot) were calculated as phospho-p65/GAPDH ratios and expressed as fold change from healthy media control. Data are mean ± SEM, $n = 15$ (healthy controls and COPD patients) or 5 (healthy smokers). $^{*}P \leq 0.05$ versus respective uninfected media control, $^{+}P \leq 0.05$ versus infected or uninfected healthy controls. Statistical differences were determined with one-way ANOVA followed by Bonferroni post-test.

COPD as previously described (27, 28, 32–35, 39). Mice were then infected with IAV A/PR/8/34, and viral titers, airway inflammation (histopathological score), and inflammatory and antiviral cytokines were determined at 7 days postinfection (dpi) (Figure 2A). Infection in Air-exposed controls leads to virus replication (Figure 2B) that was accompanied by significant airway inflammation (histopathological score, Supplemental Figure 1B). Infection in Smk-exposed mice resulted in a significantly higher

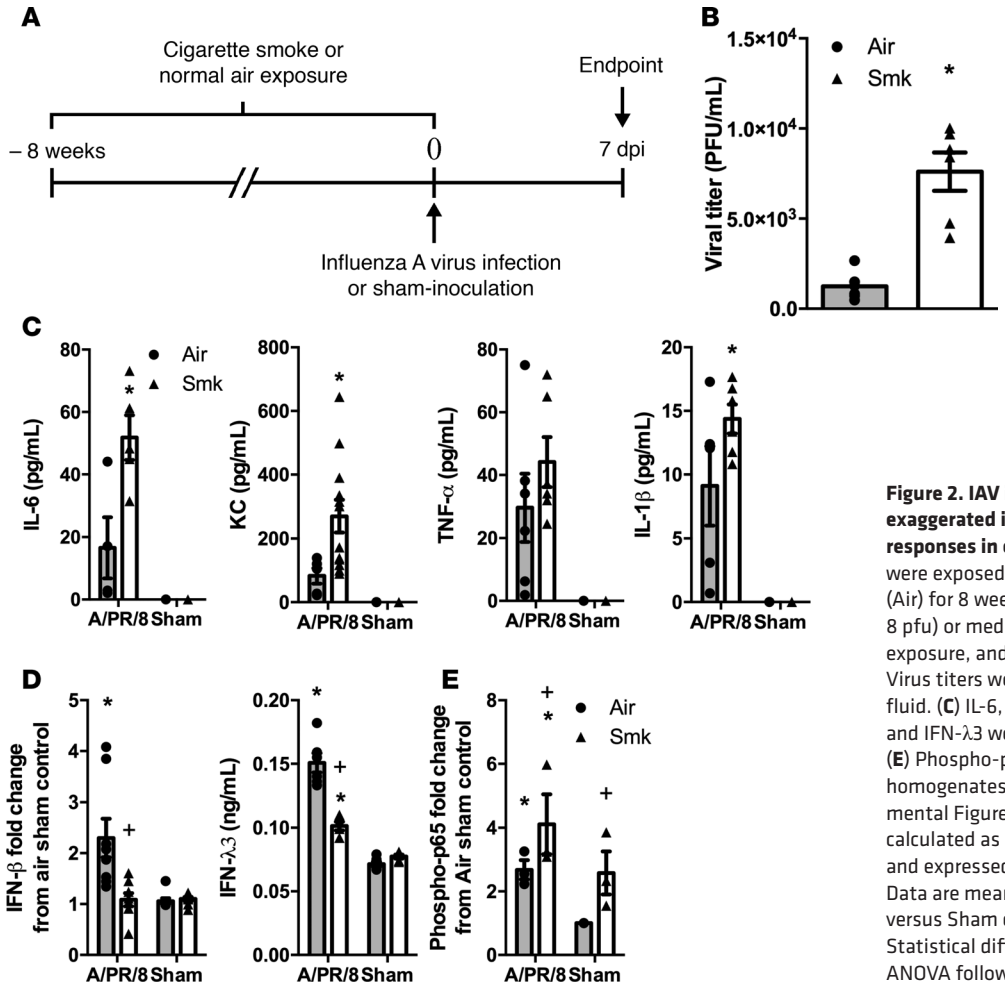

Figure 2. IAV infection is more severe and results in exaggerated inflammatory and impaired antiviral responses in experimental COPD. (**A**) BALB/c mice were exposed to cigarette smoke (Smk) or normal air (Air) for 8 weeks, infected with IAV H1N1 (A/PR/8/34, 8 pfu) or media (Sham) on the last day of smoke exposure, and sacrificed 7 days postinfection (dpi). (**B**) Virus titers were measured in bronchoalveolar lavage fluid. (**C**) IL-6, KC, TNF-α, and IL-1β and (**D**) IFN-β and IFN-λ3 were assessed in lung homogenates. (**E**) Phospho-p65 protein was determined in lung homogenates. Densitometry results (from Supplemental Figure 1D, representative immunoblot) were calculated as phospho-p65 or IFN-β/β-actin ratios and expressed as fold change from Air sham control. Data are mean ± SEM, n = 6–8 per group. $^{*}P \le 0.05$ versus Sham control, $^{+}P \le 0.05$ versus Air control. Statistical differences were determined with one-way ANOVA followed by Bonferroni post-test.

virus titer (4-fold) and airway histopathological score (3-fold) compared with Air-exposed mice. In support of these data, the levels of the proinflammatory cytokines/chemokines IL-6, KC (mouse equivalent of CXCL-8), TNF-α, and IL-1β were also increased by infection in Air-exposed groups and to a greater extent in Smk-exposed groups (Figure 2C). Antiviral cytokines were increased in infected Air-exposed controls but were either not induced (IFN-β) or were induced to a much reduced level (IFN-λ3) in infected Smk-exposed groups (Figure 2D). The exaggerated release of proinflammatory cytokines was associated with significantly increased levels of phospho-p65 protein in infected Smk-exposed compared with Air-exposed controls (Figure 2E and Supplemental Figure 1C). In all experiments, ultraviolet-inactivated virus did not have any effects compared with media controls (data not shown).

Taken together, these human ex vivo and experimental in vivo data demonstrate that IAV infections result in increased airway inflammation and proinflammatory and antiviral responses. However, COPD is associated with exaggerated inflammation and reduced antiviral responses, leading to increased virus replication.

A20 is an important negative regulatory of NF-κB–mediated inflammatory but not antiviral responses, and its expression is reduced in human COPD and experimental COPD. We have previously shown that A20 is an important negative regulator of NF-κB activation (11–14), but its roles during IAV infection and whether it also regulates the induction of type I and III IFNs is unclear. We hypothesized that A20 protein expression would be downregulated and would contribute to the increased activation of NF-κB in response to IAV infection in COPD. IAV infection led to a significant induction of A20 protein at 6 hours and 24 hours in healthy and smoker controls, but this increase was impaired in COPD pBECs (Figure 3A and Supplemental Figure 2A). Similarly in Smk-exposed mice, A20 protein expression was reduced in airway epithelial cells compared with Air-exposed controls (Supplemental Figure 2B).

We then investigated if A20 was important in NF-κB–mediated inflammatory responses and if exaggerated p65 activation was the direct result of reduced A20 protein levels during infection in COPD pBECs.

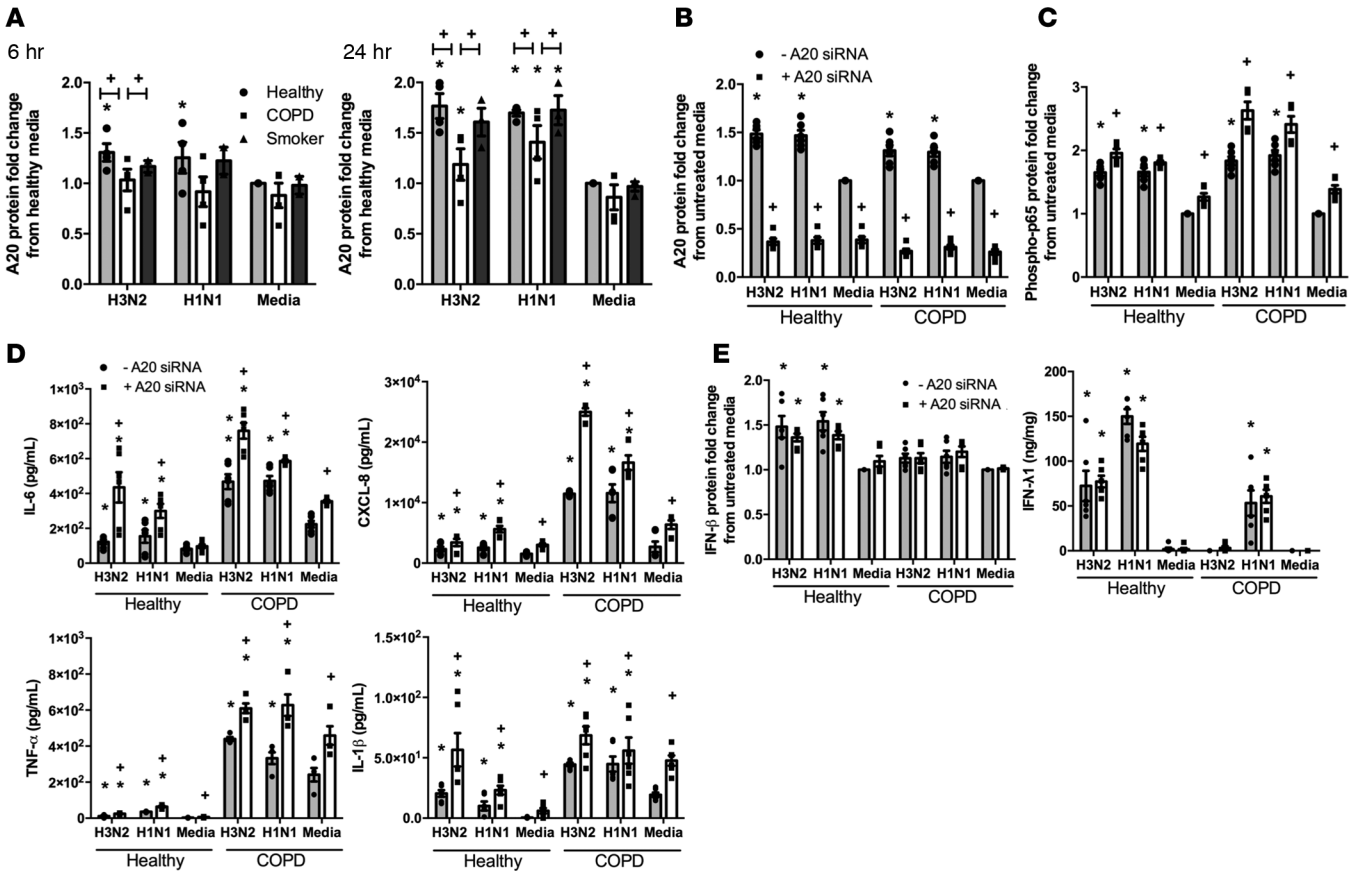

Figure 3. A20 expression is reduced and negatively regulates inflammatory but not antiviral responses in pBECs from patients with COPD. (**A**) pBECs were infected with human IAV H3N2 or H1N1, and the protein levels of A20 were determined at 6 hours and 24 hours. Densitometry results (from Supplemental Figure 2A, representative immunoblot) were calculated as A20 or phospho-p65/GAPDH ratios and expressed as fold change from healthy media control. Data are mean ± SEM, $n = 15$ per group. $^*P \leq 0.05$ versus respective uninfected media control, $^+P \leq 0.05$ versus healthy control. A20 expression was inhibited with a specific siRNA, pBECs were infected with IAVs, and protein levels of (**B**) A20; (**C**) phospho-p65; (**D**) cytokines/chemokines IL-6, CXCL-8, TNF-α, and IL-1β; and antiviral (**E**) IFN-β and IFN-λ1 were measured 24 hours later. Densitometric ratios (from Supplemental Figure 2C, representative immunoblot) were expressed as fold change from untreated media control. Data are mean ± SEM, $n = 3$ per group. $^*P \leq 0.05$ versus untreated, uninfected media control, $^+P \leq 0.05$ versus untreated infected or uninfected control. Statistical differences were determined with one-way ANOVA followed by Bonferroni post-test.

We inhibited A20 expression using A20-specific siRNA 24 hours before infection and measured the activation of p65 and the production of proinflammatory cytokines/chemokines 24 hours after infection. Inhibition of A20 expression (Figure 3B and Supplemental Figure 2C) resulted in significant increases in the protein levels of phospho-p65 (Figure 3C and Supplemental Figure 2C) and proinflammatory cytokines/chemokines IL-6, CXCL-8, TNF-α, and IL-1β (Figure 3D) compared with untreated controls, whether pBECs were infected or not. Conversely, ectopic expression (ecto-expression) using a pcDNA-A20 expression vector reduced the phosphorylation of p65 (Supplemental Figure 2D). Nevertheless, inhibition or ecto-expression of A20 did not affect IFN-β and IFN-λ1 induction (Figure 3E and Supplemental Figure 2D). siRNA negative control or control vector did not affect the induction of A20 or phospho-p65 protein (Supplemental Figure 2, E and F).

Collectively, these data indicate that A20 is an important negative regulator of NF-κB but is dispensable in the induction of type I and III IFNs. A20 protein expression is dysregulated in COPD.

Elevated miR-125a and -b levels decrease A20 levels, increase inflammation and impair antiviral responses in COPD pBEC and experimental COPD. miR-125a and -b have recently been shown to directly target and inhibit A20 expression (16), but their roles during IAV infection and in COPD are unknown. Thus, we measured the levels of miR-125a and -b induced by IAV infection. H3N2 and H1N1 infections resulted in significant increases in the levels of these miRNAs at 24 hours in pBECs from all groups (Figure 4A). However, their levels were substantially greater at baseline and during infection (2- to 4-fold) in COPD pBECs compared with healthy controls. We then confirmed the direct link between increased miR-125a and -b levels and

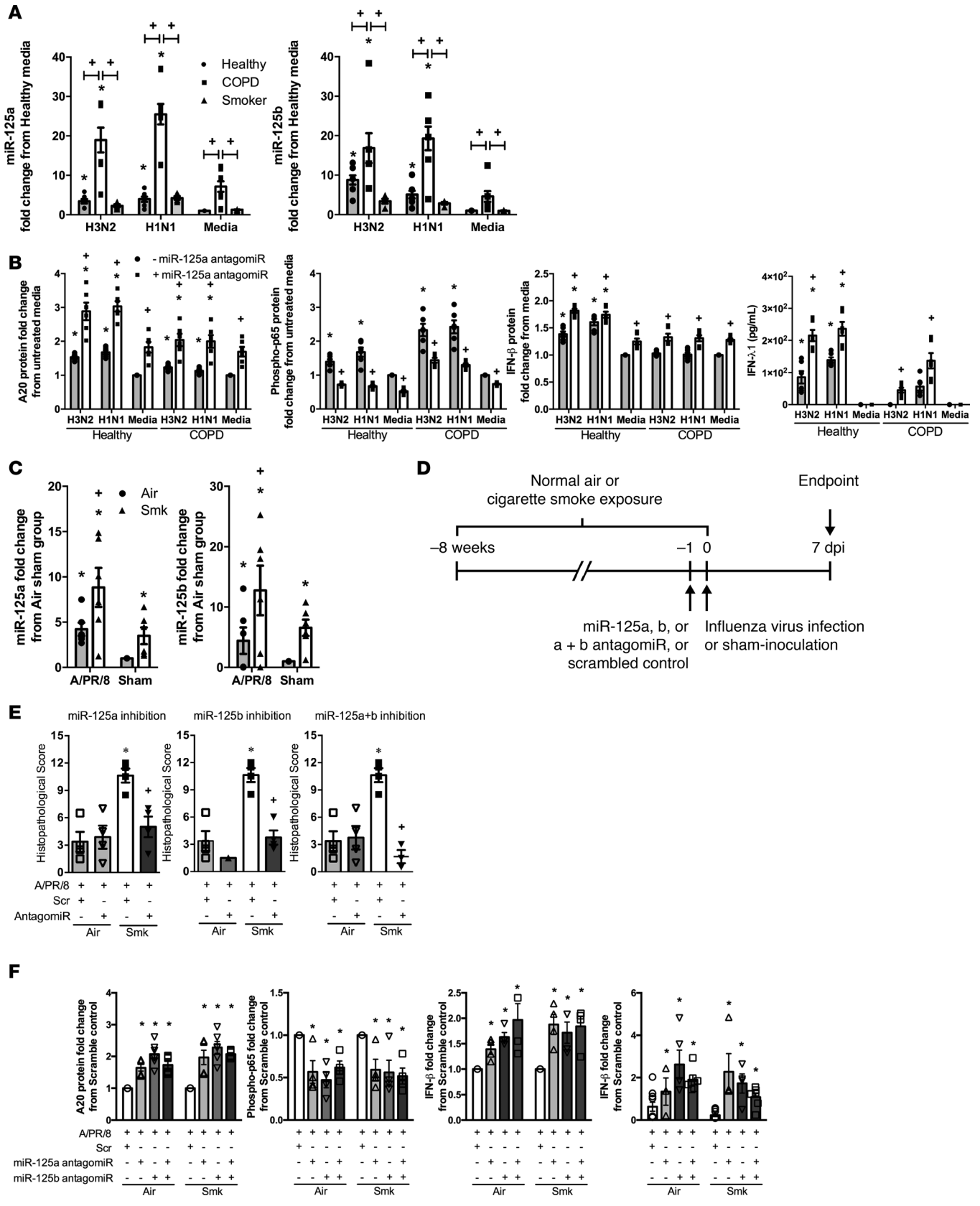

Figure 4. IAV infection increases the levels of miR-125 and -b that suppress the production of A20, increase inflammatory responses, and reduce antiviral responses in human COPD pBECs and experimental COPD. pBECs were infected with human IAV H3N2 or H1N1, and (**A**) miR-125a and -b levels were assessed at 24 hours. Data are mean ± SEM, $n = 15$ per group. *$P \leq 0.05$ versus uninfected media control, $^{+}P \leq 0.05$ versus healthy or smoker control. (**B**) pBECs were treated with miR-125a or -b antagomir and were infected, and the levels of A20, phospho-p65, IFN-β, and IFN-λ1 were assessed.

Densitometry results (Supplemental Figure 3B, representative immunoblot) were calculated as A20 or phospho-p65/GAPDH ratios and expressed as fold change from untreated, uninfected control. Data are mean ± SEM, n = 3 per group. *$P \leq 0.05$ versus untreated, uninfected media control; $^{+}P \leq 0.05$ versus untreated infected or uninfected group. (**C**) BALB/c mice were exposed to cigarette smoke (Smk) or normal air (Air) for 8 weeks, inoculated with IAV H1N1 (A/PR/8/34, 8 pfu) or media (Sham) on the last day of smoke exposure, and sacrificed 7 days postinfection (dpi). The levels of miR-125a and -b were measured. Data are mean ± SEM, n = 6–8 per group. *$P \leq 0.05$ versus Sham group, $^{+}P \leq 0.05$ versus Air-infected or uninfected group. (**D**) In other groups, on the last day of smoke exposure, mice were treated with miR-125a or -b antagomir alone or in combination and infected with IAV, and (**E**) airway histological scores were assessed. Data are mean ± SEM, n = 6–8 per group. *$P \leq 0.05$ versus infected and scrambled treated Air controls, $^{+}P \leq 0.05$ versus infected and scramble-treated Smk group. (**F**) The protein levels of A20, phospho-p65, and IFN-β in lung homogenates were also measured. Densitometry results (Supplemental Figure 4D) were calculated as A20 or phospho-p65/β-actin ratios and expressed as fold change from untreated, uninfected control. Data are mean ± SEM, n = 6–8 per group. *$P \leq 0.05$ versus infected scrambled-treated Air group, $^{+}P \leq 0.05$ versus infected scrambled Smk group. Statistical differences were determined with one-way ANOVA followed by Bonferroni post-test.

reduced A20 protein induction using specific antagomirs and mimetics. pBECs were pretreated with either miR-125a or -b specific antagomirs or mimetics for 24 hours before infection, and A20, phospho-p65, inflammatory, and antiviral cytokines were assessed 24 hours after infection. Antagomir treatment inhibited miR-125a or -b expression (Supplemental Figure 3A), and this resulted in significant increases in A20 protein production, reduced phosphorylation of p65, subsequent induction of proinflammatory cytokines/chemokines, and enhanced antiviral IFN-β and -λ1 responses (Figure 4B and Supplemental Figure 3, B–E) compared with untreated controls. Conversely, miR-125a or -b mimetics decreased A20 protein induction, increased phospho-p65protein levels, and reduced IFN-β responses (Supplemental Figure 3F). Treatment with scrambled miRNA or mimetic controls did not affect A20, phospho-p65, or IFN-β production (Supplemental Figure 3, G and H).

We then assessed whether similar events occurred in vivo. IAV infection significantly increased the levels of miR-125a and -b in both groups, with the levels in Smk group significantly higher compared with Air-exposed controls (Figure 4C). We then inhibited miR-125a or -b before and during infection (Figure 4D). We also extended the ex vivo data by inhibiting both miR-125a and -b together. Treatment with miR-125a or -b antagomir, alone or in combination, reduced histopathological scores (Figure 4E and Supplemental Figure 4A) and improved lung function (reduced lung volume determined during a pressure-volume loop maneuver) in Air- and Smk-exposed groups compared with infected scrambled antagomir-treated controls (Supplemental Figure 4B). Inhibition of miR-125a, -b, or -a and -b, also increased A20 protein expression in the airway epithelium and decreased the levels of phospho-p65 compared with the controls (Figure 4F and Supplemental Figure 4, C and D). Importantly, while we could only detect reductions in TNF-α and KC with combined treatment (Supplemental Figure 4E), antagomir treatment, either alone or in combination, also significantly increased IFN-β and IFN-λ3 protein induction (Figure 4F and Supplemental Figure 4D).

Collectively, these data show that miR-125a and -b are directly involved in the regulation of both inflammatory cytokines — through the control of A20 — and antiviral cytokine production through an unknown target.

miR-125a and -b target MAVS. To determine the mechanism of miR-125a– and -b–mediated regulation of antiviral IFN-β/λ, we performed miRNA prediction analysis using TargetScan (www.targetscan.org). miR-125a and -b have a putative binding site in the 3′-UTR of human and mouse *MAVS* (Figure 5, A and B). To examine these putative interactions, we first assessed the protein levels of MAVS in pBECs. MAVS protein levels were significantly increased 24 hours after IAV infection in healthy control and smoker pBECs, but notably not in COPD pBECs Figure 5C and Supplemental Figure 5A). Similarly, infection in Smk-exposed mice was also associated with significantly impaired production of MAVS compared with infected Air-exposed controls at 7 dpi (Figure 5D and Supplemental Figure 5B).

To confirm the potential interaction of miR-125a or -b and MAVS, we cloned the putative binding region of miR-125a and -b in WT (MAVS-WT) or mutant (MAVS-MT) *MAVS* 3′-UTR into a luciferase reporter construct. The construct was cotransfected into HEK293 cells along with miR-125a or -b mimetics, or scrambled controls, and then luciferase activity was assessed. Cotransfection of miR-125a or miR-125b mimetics with MAVS-WT resulted in a significant decrease in luciferase activity compared with scrambled controls (Figure 5E). There was no reduction in activity with cotransfection with MAVS-MT. We then determined if *MAVS* gene is present with the miR-125a or -b mimetics in the silencing complex. To do this, we immunoprecipitated Argonaute 2 (Ago2), a core component of RNA-induced silencing complex (RISC) that binds to the miRNAs and their target mRNA, with a specific antibody and detected the presence of both

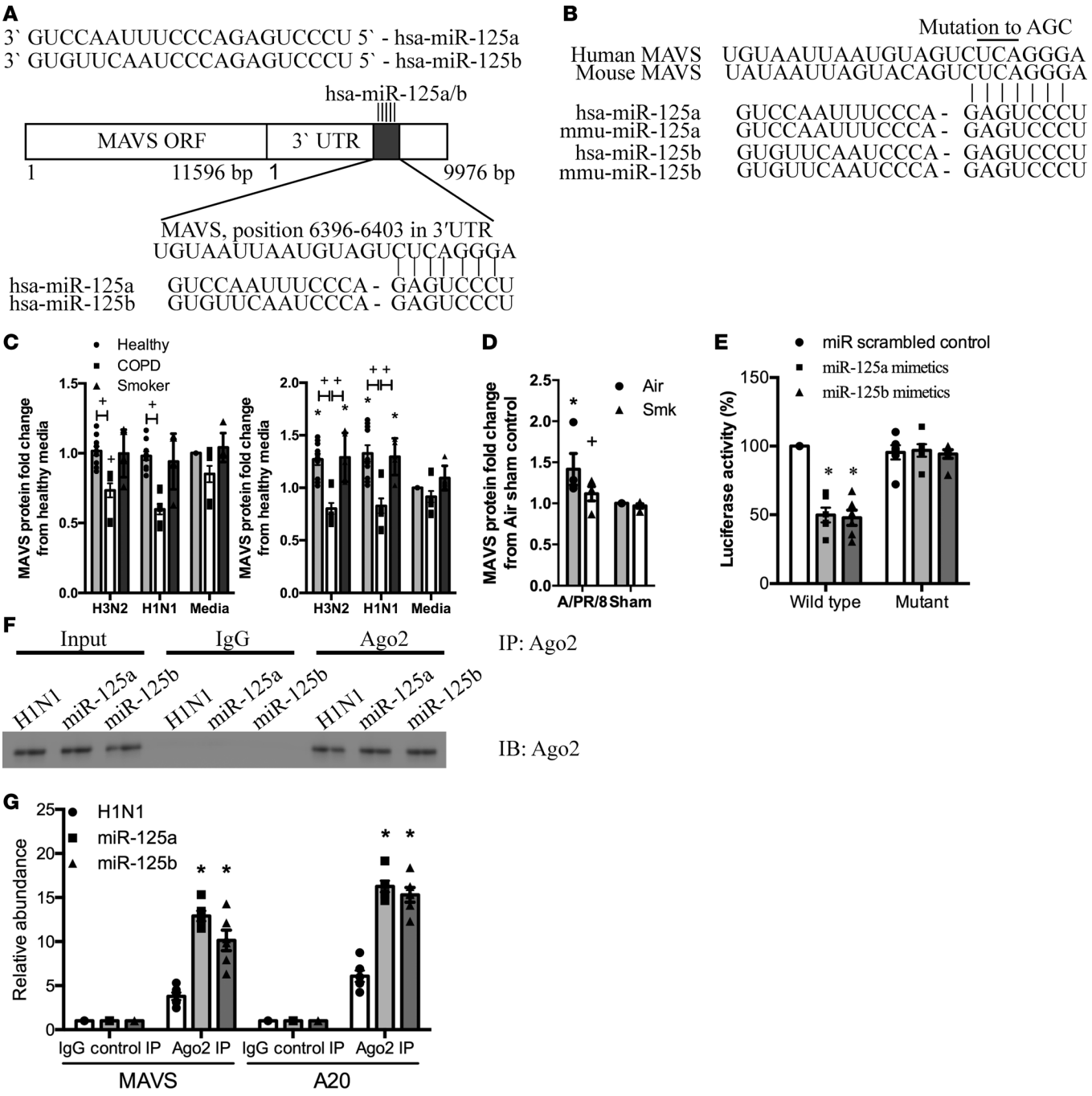

Figure 5. miR-125a and -b target a functional binding site of the 3′-UTR of the mRNA of MAVS to suppress its expression. (**A**) Representation of *MAVS* gene structure and location of miR-125a and -b binding site. (**B**) The binding site on 3′-UTR of *MAVS* is 100% conserved between human and mouse *MAVS*. (**C**) pBECs were infected with H3N2 or H1N1, and MAVS protein was detected at 6 hours (left) and 24 hours (right). Densitometry results (Supplemental Figure 5A, representative immunoblot) were calculated as MAVS/GAPDH ratios and expressed as fold change from untreated, uninfected controls. Data are mean ± SEM, n = 15 per group. *$P \leq 0.05$ versus uninfected healthy or smoker controls, $^{+}P \leq 0.05$ versus infected or uninfected healthy controls. (**D**) BALB/c mice were exposed to cigarette smoke (Smk) or normal air (Air) for 8 weeks, inoculated with IAV H1N1 (A/PR/8/34, 8 pfu) or media (Sham) on the last day of smoke exposure, and sacrificed 7 days postinoculation (dpi). The levels of MAVS protein were measured in lung homogenates. Densitometry results (Supplemental Figure 5B, representative immunoblot) were calculated as MAVS/β-actin ratios in mouse and expressed as fold change from untreated, uninfected controls. Data are mean ± SEM, n = 6 per group. *$P \leq 0.05$ versus Sham-treated controls, $^{+}P \leq 0.05$ versus infected Air controls. (**E**) The miR-125a and -b binding site on 3′-UTR was cloned into a pMIR luciferase reporter construct and transfected into HEK293 cells with miR-125a or -b mimetics. The luciferase reporter assay was performed to determine binding. Data are mean ± SEM, n = 3 per group.*$P \leq 0.05$ versus miRNA scrambled controls. (**F**) Ago2 was immunoprecipitated from miR-125a or -b mimetic-transfected HEK293, and (**G**) A20 and MAVS mRNA was detected by qPCR in Ago2-immunoprecipitate. Data are mean ± SEM, n = 3 per group. *$P \leq 0.05$ versus IgG control IP. Statistical differences were determined with one-way ANOVA followed by Bonferroni post-test.

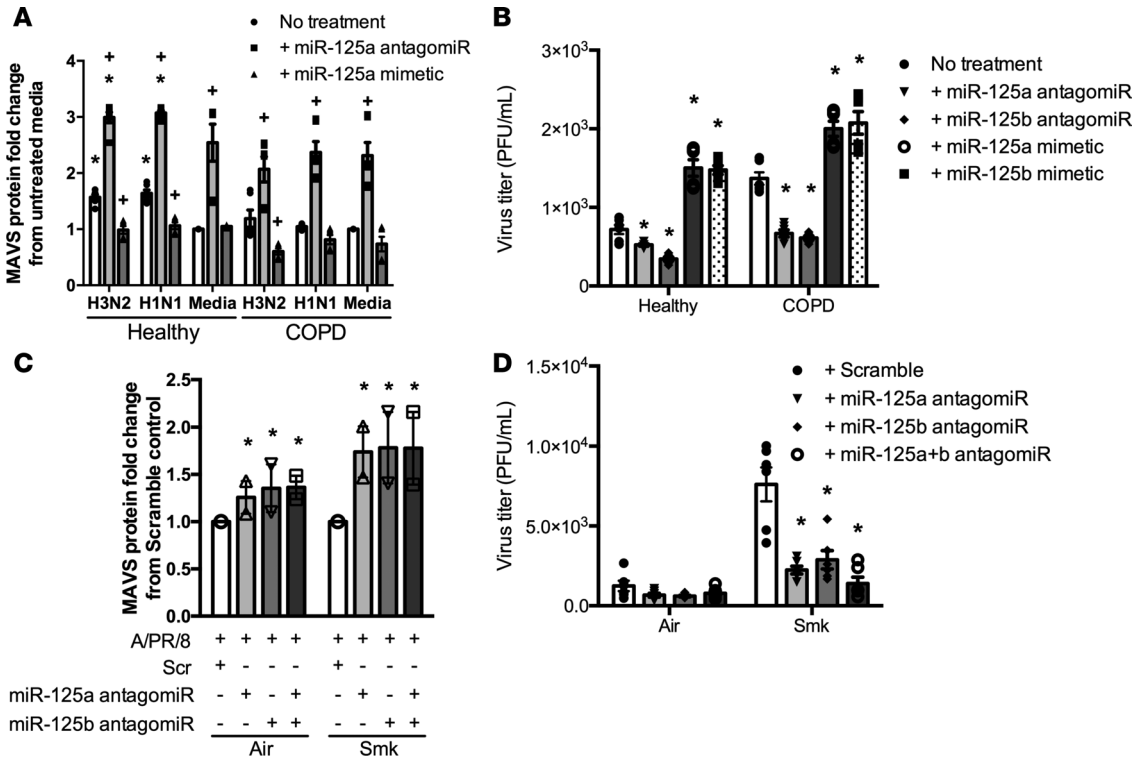

Figure 6. miR-125a and -b suppress the induction of MAVS and promote virus replication in human COPD pBECs and experimental COPD. (**A**) miR-125a and -b antagomir or mimetics were added to pBECs before infection with human IAV H3N2 or H1N1, and mitochondrial antiviral signaling (MAVS) protein were assessed 24 hours after infection. Densitometry results (Supplemental Figure 6A, representative immunoblot) were calculated as MAVS/GAPDH ratios and expressed as fold change from untreated, uninfected controls. Data are mean ± SEM, $n = 3$. $^*P \le 0.05$ versus untreated, uninfected media controls; $^+P \le 0.05$ versus untreated, infected or uninfected controls. (**B**) Virus replication was also measured. Data are mean ± SEM, $n = 3$. $^*P \le 0.05$ versus untreated, infected controls. (**C**) BALB/c mice were exposed to cigarette smoke (Smk) or normal air (Air) for 8 weeks, treated with mir125a and/or -b antagomir, infected with IAV H1N1 (A/PR/8/34, 8 pfu) or media (Sham) on the last day of smoke exposure, and sacrificed 7 days postinoculation (dpi). MAVS protein was measured. Densitometry results (Supplemental Figure 6C, representative immunoblot) were calculated as MAVS/β-actin ratios and expressed as fold change from untreated, uninfected controls. Data are mean ± SEM, $n = 6$. $^*P \le 0.05$ versus infected, scramble treated Air or Smk controls. (**D**) Virus replication was assessed. Data are mean ± SEM, $n = 6$. $^*P \le 0.05$ versus infected, scramble-treated controls. Statistical differences were determined with one-way ANOVA followed by Bonferroni post-test.

A20 and *MAVS* by qPCR, which could not be detected with immunoprecipitation with IgG control (Figure 5, F and G). This confirmed that miR-125a and -b directly bind to the endogenous 3′-UTR of *MAVS*.

miR-125a and -b targeting of MAVS regulates antiviral responses in COPD pBEC and experimental COPD. We then investigated whether inhibition of miR-125 has a functional outcome. We showed that miR-125a and -b antagomir treatment led to significant increases in MAVS (Figure 6A and Supplemental Figure 6, A and B), IFN-β, and IFN-λ1 protein induction (Figure 4B and Supplemental Figure 3C) and reduced viral replication in both healthy and control pBECs (Figure 6B). In contrast, mimetics suppressed the induction of antiviral cytokines and increased virus titers (Supplemental Figure 3F). Similarly in Smk-exposed mice, inhibition of miR-125a, -b, or -a and -b resulted in increased induction of MAVS (Figure 6C and Supplemental Figure 6C), IFN-β, and IFN-λ3 (Figure 4F and Supplemental Figure 4, D and E) and inhibited virus replication (Figure 6D).

Collectively, these data demonstrate that miR-125a and -b negatively regulate MAVS expression, suppress the induction of IFN-β/λ, and may potentially be targeted therapeutically in the prevention and/or treatment of IAVs and COPD.

Discussion

Here, we discovered that IAV infections induce airway inflammation and antiviral responses; however, in COPD, pBECs and experimental COPD inflammatory responses and activation of NF-κB are exaggerated, but antiviral responses are impaired. We show that A20 is a negative regulator of NF-κB–mediated induction of inflammatory but not antiviral cytokines and that A20 protein levels were impaired in

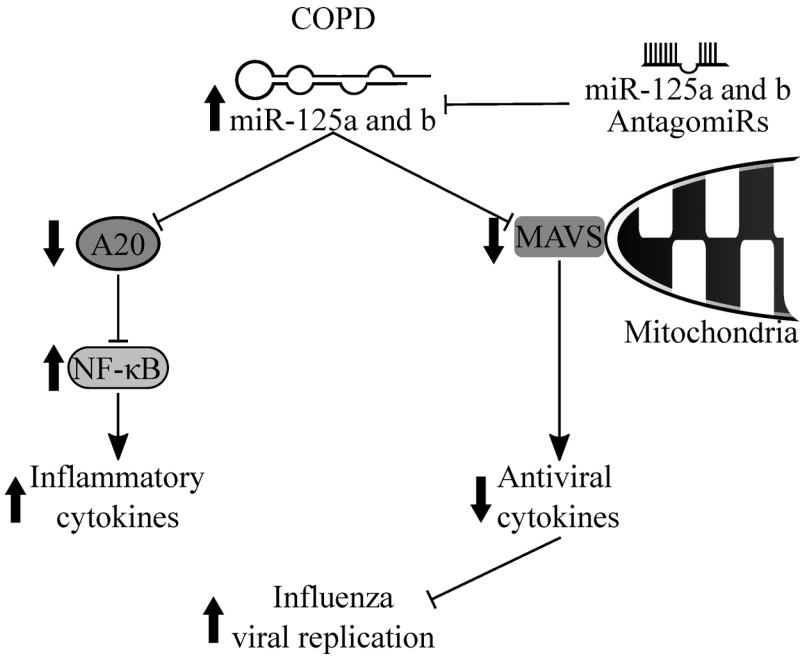

Figure 7. Roles of miR-125a and -b in the regulation of inflammatory and antiviral responses in IAV infection. Increased levels of miR-125a and -b, for example in COPD, reduce the protein expression of A20 that results in uncontrolled NF-κB activation, leading to exaggerated induction of proinflammatory cytokines. miR-125a and -b also target and reduce MAVS and antiviral type I and III IFN production. Inhibition of miR-125a and -b enhances MAVS and antiviral responses, and it suppresses viral infection.

COPD. The impaired induction of A20 and antiviral responses in COPD were attributed to increased expression of miR-125a and -b. Elevated levels of these miRNAs suppressed A20 expression, leading to heightened NF-κB activity and inflammation and reduced antiviral responses. Inhibition with miR-125a and -b antagomirs increased A20 levels and reduced NF-κB activity, and also promoted IFN production. We then demonstrated that miR-125a and -b modulated IFN induction by targeting MAVS translation. MAVS protein levels were reduced in COPD but could be increased with specific miR-125a and -b antagomir treatment that also induced IFN production. Thus, IAV infection induces the expression of miR-125a or -b that suppresses A20 and MAVS, in turn promoting NF-κB–induced inflammation and attenuating antiviral IFN production, respectively, increasing viral replication. All these events are exaggerated in COPD (Figure 7).

IAV is a major infectious pathogen that poses serious health concerns worldwide. Infections, particularly with highly pathogenic influenza viruses, cause severe airway inflammation and a cytokine storm with high morbidity and mortality. COPD is a major global health problem that is underpinned by exaggerated inflammatory responses in the airways (40). IAV infections frequently result in acute exacerbations of COPD, leading to accelerated declines in lung function (41, 42) and increased mortality (20). The mechanisms of exaggerated inflammation and severe outcomes in COPD are poorly understood, and there are no effective therapies for these events.

Here, we show that IAV-mediated inflammatory response are dampened with ectopic expression of A20 that reduces NF-κB activity and inflammatory responses, without affecting type I and III IFN responses. A20 is a deubiquitinating enzyme that degrades RIP1, inhibits NF-κB activation (13), and has been shown to suppress the induction of IFN-β (43). We found that A20 modulated NF-κB activity and inflammation, but it did not affect type I and III IFNs production.

Consistent with our previous findings (27), IAV infections in COPD pBECs and experimental COPD led to heightened inflammation and production of inflammatory cytokines but impaired antiviral responses (IFN-β and IFN-λ), which were associated with greater viral replication. Increased inflammation, inflammatory cytokines, and activation of NF-κB are well known in COPD (24, 44). Here, we show that these are the result of reduced induction of A20, leading to uncontrolled activation of NF-κB and subsequent induction of inflammatory cytokines. A20 is a pleiotropic protein involved in various ubiquitin-dependent pathways, including NF-κB (16) and MAPK pathway (45), and has also been shown to negatively regulate type I IFN inductions (43, 46, 47). Surprisingly, inhibition or ectopic expression of A20 did not affect IFN-β production. The precise roles of A20 during viral infections, therefore, require further investigation. We could not rule out that other factors may also contribute to the regulation of A20 expression and of NF-κB activity, including other unidentified miRNAs, which may also be dysregulated in COPD.

Forced expression of A20 may be a novel therapeutic option that reduces IAV-mediated inflammation and cytokine storm, particularly from high pathogenic IAVs, such as H5N1, or in COPD where airway inflammation is already persistently heightened.

The lack of the induction of A20 protein during IAV infection in COPD was attributed to increased levels of miR-125a and -b. These miRNAs downregulate A20 expression by directly binding to its 3′-UTR,

Table 1. Subject characteristics

	Healthy	COPD	Smoker	*P* value
n	15	15	5	NA
Sex (male/female ratio)	1.14	1.2	1.5	$P = 0.6$
Mean age (SD)	62 (9.9)	68 (4.1)	64.33 (12.82)	$P = 0.06$
Mean FEV_1 (SD)[A]	105% (13.5)	40% (7.75)	97.66% (12.66)	$P < 0.001$
FEV_1/FVC ratio (SD)[A]	886 (14.50)	40.20 (13.50)	77.80 (12.28)	$P < 0.001$
Cigarette (packs/year; SD)	0	53.70 (15.90)	30 (17.32)	$P < 0.001$
Years abstinent (SD)	0	13.0 (4.64)	0	NA
ICS (percent treated)	0	Seretide (10%) Spiriva (10%) Tiotropium (10%) Spiriva/Salbutamol (10%) Seretide/Tiotropium (20%) Seretide/Tiotropium/Ventolin (20%) Seretide/Spiriva/Ventolin (20%)	0	NA

[A]FEV_1 and FEV_1/FVC ratios are % predicted values. FEV_1 is the forced expiratory volume in 1s expressed as a percentage of the predicated value. FVC is forced vital capacity. The statistical analysis used was ANOVA for multiple groups. NA, not applicable.

leading to constitutive activation of NF-κB (16). We found that heightened levels of miR-125a or -b resulted in increased activation of NF-κB in COPD. Inhibition of miR-125a or -b in both healthy and COPD pBECs and in experimental COPD increased A20 protein levels and reduced NF-κB activation during IAV infection.

We also found that miR-125a and -b modulated the induction of type I and III antiviral IFNs. This occurred by the direct targeting of MAVS 3′-UTR, therefore downregulating the subsequent induction of IFN-β and IFN-λ. MAVS is an important adaptor protein on mitochondria that facilitates the production of IFNs (8); however, there was an impaired induction of MAVS by IAV infections in COPD pBECs and in experimental COPD. Inhibition of miR-125a and/or -b increased the levels of MAVS and antiviral IFNs, which led to reduced virus replication both in vivo and in vitro. Interestingly, antagomirs against miR-125a and/or -b in experimental COPD partially reduced the release of inflammatory cytokines and substantially suppressed virus replication. This may indicate that miR-125a and -b may preferentially target MAVS over A20 during IAV infection in COPD, although such binding preferences of miRNAs have not been widely investigated. Furthermore, as MAVS is transcriptionally driven by IFN-sensitive response element (ISRE) as part of the ISGs (48), and miR-125a or -b have been reported to be induced by NF-κB (49), it is possible that reduced MAVS partly attributed to impaired IFNs in COPD; with enhanced expression of miR-125a or -b (NF-κB–inducible), this then leads to a continuous cycle of exaggerated inflammation and impaired antiviral immunity in COPD.

Although miR-125a or -b appear to be NF-κB inducible, the exact molecular mechanisms of enhanced miR-125a or -b expression in COPD require further investigation. In colorectal cancer tissues, the levels of miR-125a have been shown to be reduced, which is associated with hypermethylation at the CpG island within the promoter region of miR-125a (50). Similarly, in breast cancer cell lines, reduced miR-125a has also been shown to be associated with trimethylation at H3K9 and H3K27 at the promoter region of miR-125a (51). It is therefore possible that the methylation status of miR-125a or -b promoter site is altered in COPD, leading to increased expression of miR-125a or -b. Nevertheless, our data also demonstrate that specific inhibition of miR-125a or -b may be a novel therapeutic option against IAV infections and for those most vulnerable.

Cigarette smoke is the major risk factor for COPD. Acute exposure results in oxidative stress and NF-κB activation (52–54). However, the effects we have observed in COPD appear to be independent of acute exposure to cigarette smoking, as the pBECs obtained from subjects with COPD were all abstinent from smoking for at least 10 years. It is likely that chronic exposure progressively leads to persistent induction of miR-125a and -b and NF-κB activation (55, 56), which then reduces the induction of A20 and MAVS in COPD.

Collectively, our results demonstrate that A20 regulates NF-κB activation and, subsequently, the production of inflammatory cytokines, but not antiviral IFNs. COPD pBECs and mice with experimental COPD responded to IAV infection with an exaggerated inflammatory but impaired antiviral responses. Increased levels of miR-125a and -b by IAV and in COPD suppressed protein inductions of A20 and

MAVS, leading to heightened airway inflammation and reduced IFN production. Inhibition of miR-125a and -b reduced the induction of inflammatory cytokines and enhanced antiviral responses to IAV infection in both healthy and COPD states. This study therefore identifies a potential therapeutic target for IAV infection in general and in COPD.

Methods

Ex vivo. COPD patients (10) and healthy nonsmoking (10) and smoking (5) controls were recruited, and their characteristics are shown in Table 1. Subject recruitment, viruses, cell culture and viral infection, A20 plasmid, siRNA, miR-125a and -b antagomir/mimetic treatment, cloning and mutagenesis of miR-125a and -b binding sites in MAVS 3′-UTR, reporter assays, immunoblotting, cytometric bead array, immunoprecipitation, miRNA extraction and analysis, and statistical tests were performed as previously described and/or as in Supplemental Methods (27, 31, 57, 58).

In vivo. Experimental COPD and influenza infection were induced; miR-125a and -b were inhibited using specific antagomirs; and histopathology, IHC, immunoblotting, and cytometric bead array and data analyses were performed as previously described and/or as in Supplemental Methods (33, 35, 39, 59–67).

Statistics. When data were normally distributed, they were expressed as mean ± SEM. Data were analyzed using nonparametric equivalents and summarized using the median and interquartile range (IQR) when non-normally distributed. Multiple comparisons were first analyzed by the Kruskal Wallis test and then by individual testing, if significant. $P < 0.05$ was considered significant.

Study Approval. All procedures were approved by The University of Newcastle Human and Animal Ethics Committees.

Author contributions

ACYH conceived and designed the study. ACYH and KN performed all in vitro experiments. KD, TJH, and PMN performed all in vivo experiments. ACYH, KD, MRS, TJH, PMN, KN, NZ, STG, KJB, PSF, PMH, and PAW participated in the completion of the manuscript.

Acknowledgments

This study is funded by National Health and Medical Research Council of Australia (grant no. 1045762) and University of Newcastle (grant no. 1300661). The authors thank Kristy Wheeldon and Nathalie Kiaos for technical assistance with in vivo protocols.

Address correspondence to: Alan Hsu or Phil Hansbro, Priority Research Centre for Healthy Lungs, Hunter Medical Research Institute, Lot 1 Kookaburra Circuit, New Lambton Heights, Newcastle, NSW 2305, Australia. Phone: 61.2.4042.0109; E-mail: Alan.Hsu@newcastle.edu.au (A. Hsu); Philip.Hansbro@newcastle.edu.au (P. Hansbro).

1. Hallstrand TS, Hackett TL, Altemeier WA, Matute-Bello G, Hansbro PM, Knight DA. Airway epithelial regulation of pulmonary immune homeostasis and inflammation. *Clin Immunol*. 2014;151(1):1–15.
2. Hsu AC, See HV, Hansbro PM, Wark PA. Innate immunity to influenza in chronic airways diseases. *Respirology*. 2012;17(8):1166–1175.
3. Chaouat A, et al. Role for interleukin-6 in COPD-related pulmonary hypertension. *Chest*. 2009;136(3):678–687.
4. Meylan E, et al. RIP1 is an essential mediator of Toll-like receptor 3-induced NF-kappa B activation. *Nat Immunol*. 2004;5(5):503–507.
5. Monks BG, Martell BA, Buras JA, Fenton MJ. An upstream protein interacts with a distinct protein that binds to the cap site of the human interleukin 1 beta gene. *Mol Immunol*. 1994;31(2):139–151.
6. Tate MD, Ioannidis LJ, Croker B, Brown LE, Brooks AG, Reading PC. The role of neutrophils during mild and severe influenza virus infections of mice. *PLoS ONE*. 2011;6(3):e17618.
7. Hashimoto Y, Moki T, Takizawa T, Shiratsuchi A, Nakanishi Y. Evidence for phagocytosis of influenza virus-infected, apoptotic cells by neutrophils and macrophages in mice. *J Immunol*. 2007;178(4):2448–2457.
8. Seth RB, Sun L, Ea CK, Chen ZJ. Identification and characterization of MAVS, a mitochondrial antiviral signaling protein that activates NF-kappaB and IRF 3. *Cell*. 2005;122(5):669–682.
9. Hsu AC, et al. Critical role of constitutive type I interferon response in bronchial epithelial cell to influenza infection. *PLoS ONE*. 2012;7(3):e32947.
10. Verhelst J, Parthoens E, Schepens B, Fiers W, Saelens X. Interferon-inducible protein Mx1 inhibits influenza virus by interfering with functional viral ribonucleoprotein complex assembly. *J Virol*. 2012;86(24):13445–13455.

11. Heyninck K, et al. The zinc finger protein A20 inhibits TNF-induced NF-kappaB-dependent gene expression by interfering with an RIP- or TRAF2-mediated transactivation signal and directly binds to a novel NF-kappaB-inhibiting protein ABIN. *J Cell Biol*. 1999;145(7):1471–1482.
12. Heyninck K, Beyaert R. The cytokine-inducible zinc finger protein A20 inhibits IL-1-induced NF-kappaB activation at the level of TRAF6. *FEBS Lett*. 1999;442(2-3):147–150.
13. Grey ST, Arvelo MB, Hasenkamp W, Bach FH, Ferran C. A20 inhibits cytokine-induced apoptosis and nuclear factor kappaB-dependent gene activation in islets. *J Exp Med*. 1999;190(8):1135–1146.
14. Ferran C, et al. A20 inhibits NF-kappaB activation in endothelial cells without sensitizing to tumor necrosis factor-mediated apoptosis. *Blood*. 1998;91(7):2249–2258.
15. Foster PS, et al. The emerging role of microRNAs in regulating immune and inflammatory responses in the lung. *Immunol Rev*. 2013;253(1):198–215.
16. Kim SW, Ramasamy K, Bouamar H, Lin AP, Jiang D, Aguiar RC. MicroRNAs miR-125a and miR-125b constitutively activate the NF-κB pathway by targeting the tumor necrosis factor alpha-induced protein 3 (TNFAIP3, A20). *Proc Natl Acad Sci USA*. 2012;109(20):7865–7870.
17. World Health Organization. Chronic Obtructive Pulmonary Disease (COPD) Fact Sheet. http://www.who.int/mediacentre/factsheets/fs315/en/. Published November 2016. Accessed February 20, 2017.
18. Lopez AD, Mathers CD, Ezzati M, Jamison DT, Murray CJ. Global and regional burden of disease and risk factors, 2001: systematic analysis of population health data. *Lancet*. 2006;367(9524):1747–1757.
19. Hurst JR, et al. Susceptibility to exacerbation in chronic obstructive pulmonary disease. *N Engl J Med*. 2010;363(12):1128–1138.
20. Soler-Cataluña JJ, Martínez-García MA, Román Sánchez P, Salcedo E, Navarro M, Ochando R. Severe acute exacerbations and mortality in patients with chronic obstructive pulmonary disease. *Thorax*. 2005;60(11):925–931.
21. Seemungal T, et al. Respiratory viruses, symptoms, and inflammatory markers in acute exacerbations and stable chronic obstructive pulmonary disease. *Am J Respir Crit Care Med*. 2001;164(9):1618–1623.
22. Nath KD, et al. Clinical factors associated with the humoral immune response to influenza vaccination in chronic obstructive pulmonary disease. *Int J Chron Obstruct Pulmon Dis*. 2014;9:51–56.
23. Hurt AC, et al. Community transmission of oseltamivir-resistant A(H1N1)pdm09 influenza. *N Engl J Med*. 2011;365(26):2541–2542.
24. Di Stefano A, et al. Increased expression of nuclear factor-kappaB in bronchial biopsies from smokers and patients with COPD. *Eur Respir J*. 2002;20(3):556–563.
25. Hsu AC, Barr I, Hansbro PM, Wark PA. Human influenza is more effective than avian influenza at antiviral suppression in airway cells. *Am J Respir Cell Mol Biol*. 2011;44(6):906–913.
26. Chan MC, et al. Proinflammatory cytokine responses induced by influenza A (H5N1) viruses in primary human alveolar and bronchial epithelial cells. *Respir Res*. 2005;6:135.
27. Hsu AC, et al. Targeting PI3K-p110α Suppresses Influenza Virus Infection in Chronic Obstructive Pulmonary Disease. *Am J Respir Crit Care Med*. 2015;191(9):1012–1023.
28. Beckett EL, et al. A new short-term mouse model of chronic obstructive pulmonary disease identifies a role for mast cell tryptase in pathogenesis. *J Allergy Clin Immunol*. 2013;131(3):752–762.
29. Hsu AC, et al. Impaired Antiviral Stress Granule and IFN-β Enhanceosome Formation Enhances Susceptibility to Influenza Infection in Chronic Obstructive Pulmonary Disease Epithelium. *Am J Respir Cell Mol Biol*. 2016;55(1):117–127.
30. Tay HL, et al. Antagonism of miR-328 increases the antimicrobial function of macrophages and neutrophils and rapid clearance of non-typeable Haemophilus influenzae (NTHi) from infected lung. *PLoS Pathog*. 2015;11(4):e1004549.
31. Conickx G, et al. MicroRNA Profiling Reveals a Role for MicroRNA-218-5p in the Pathogenesis of Chronic Obstructive Pulmonary Disease. *Am J Respir Crit Care Med*. 2017;195(1):43–56.
32. Fricker M, Deane A, Hansbro PM. Animal models of chronic obstructive pulmonary disease. *Expert Opin Drug Discov*. 2014;9(6):629–645.
33. Franklin BS, et al. The adaptor ASC has extracellular and 'prionoid' activities that propagate inflammation. *Nat Immunol*. 2014;15(8):727–737.
34. Hansbro PM, et al. Importance of mast cell Prss31/transmembrane tryptase/tryptase-γ in lung function and experimental chronic obstructive pulmonary disease and colitis. *J Biol Chem*. 2014;289(26):18214–18227.
35. Haw TJ, et al. A pathogenic role for tumor necrosis factor-related apoptosis-inducing ligand in chronic obstructive pulmonary disease. *Mucosal Immunol*. 2016;9(4):859–872.
36. Mehra NK. A brief history of the Federation of Immunological Societies of Asia-Oceania (FIMSA). *Ann N Y Acad Sci*. 2013;1283:v–x.
37. Hussain S, et al. Inflammasome activation in airway epithelial cells after multi-walled carbon nanotube exposure mediates a profibrotic response in lung fibroblasts. *Part Fibre Toxicol*. 2014;11:28.
38. Higham A, Lea S, Ray D, Singh D. Corticosteroid effects on COPD alveolar macrophages: dependency on cell culture methodology. *J Immunol Methods*. 2014;405:144–153.
39. Liu G, et al. Fibulin-1 regulates the pathogenesis of tissue remodeling in respiratory diseases. *JCI Insight*. 2016;1(9):e86380.
40. Asher MI, et al. Worldwide time trends in the prevalence of symptoms of asthma, allergic rhinoconjunctivitis, and eczema in childhood: ISAAC Phases One and Three repeat multicountry cross-sectional surveys. *Lancet*. 2006;368(9537):733–743.
41. Kanner RE, Anthonisen NR, Connett JE, Lung Health Study Research Group. Lower respiratory illnesses promote FEV(1) decline in current smokers but not ex-smokers with mild chronic obstructive pulmonary disease: results from the lung health study. *Am J Respir Crit Care Med*. 2001;164(3):358–364.
42. Seemungal TA, Donaldson GC, Paul EA, Bestall JC, Jeffries DJ, Wedzicha JA. Effect of exacerbation on quality of life in patients with chronic obstructive pulmonary disease. *Am J Respir Crit Care Med*. 1998;157(5 Pt 1):1418–1422.
43. Wang YY, Li L, Han KJ, Zhai Z, Shu HB. A20 is a potent inhibitor of TLR3- and Sendai virus-induced activation of NF-kappaB and ISRE and IFN-beta promoter. *FEBS Lett*. 2004;576(1-2):86–90.
44. Barnes PJ. The cytokine network in asthma and chronic obstructive pulmonary disease. *J Clin Invest*. 2008;118(11):3546–3556.
45. Jung SM, et al. Smad6 inhibits non-canonical TGF-β1 signalling by recruiting the deubiquitinase A20 to TRAF6. *Nat Commun*.

2013;4:2562.
46. Saitoh T, et al. A20 is a negative regulator of IFN regulatory factor 3 signaling. *J Immunol*. 2005;174(3):1507–1512.
47. Maelfait J, et al. A20 (Tnfaip3) deficiency in myeloid cells protects against influenza A virus infection. *PLoS Pathog*. 2012;8(3):e1002570.
48. Rusinova I, et al. Interferome v2.0: an updated database of annotated interferon-regulated genes. *Nucleic Acids Res*. 2013;41(Database issue):D1040–D1046.
49. Lee HM, Kim TS, Jo EK. MiR-146 and miR-125 in the regulation of innate immunity and inflammation. *BMB Rep*. 2016;49(6):311–318.
50. Chen H, Xu Z. Hypermethylation-Associated Silencing of miR-125a and miR-125b: A Potential Marker in Colorectal Cancer. *Dis Markers*. 2015;2015:345080.
51. Cisneros-Soberanis F, Andonegui MA, Herrera LA. miR-125b-1 is repressed by histone modifications in breast cancer cell lines. *Springerplus*. 2016;5(1):959.
52. Kirkham PA, Barnes PJ. Oxidative stress in COPD. *Chest*. 2013;144(1):266–273.
53. Fischer BM, Pavlisko E, Voynow JA. Pathogenic triad in COPD: oxidative stress, protease-antiprotease imbalance, and inflammation. *Int J Chron Obstruct Pulmon Dis*. 2011;6:413–421.
54. Kratsovnik E, Bromberg Y, Sperling O, Zoref-Shani E. Oxidative stress activates transcription factor NF-kB-mediated protective signaling in primary rat neuronal cultures. *J Mol Neurosci*. 2005;26(1):27–32.
55. Tan G, Niu J, Shi Y, Ouyang H, Wu ZH. NF-κB-dependent microRNA-125b up-regulation promotes cell survival by targeting p38α upon ultraviolet radiation. *J Biol Chem*. 2012;287(39):33036–33047.
56. Werner SL, et al. Encoding NF-kappaB temporal control in response to TNF: distinct roles for the negative regulators Ikappa-Balpha and A20. *Genes Dev*. 2008;22(15):2093–2101.
57. Gómez FP, Rodriguez-Roisin R. Global Initiative for Chronic Obstructive Lung Disease (GOLD) guidelines for chronic obstructive pulmonary disease. *Curr Opin Pulm Med*. 2002;8(2):81–86.
58. . Workshop summary guidelines: investigative use of bronchoscopy, lavage, bronchial biopsies in asthma other airway diseases. *J Allergy Clin Immunol*. 1991;88(5):808–814.
59. Horvat JC, et al. Chlamydial respiratory infection during allergen sensitization drives neutrophilic allergic airways disease. *J Immunol*. 2010;184(8):4159–4169.
60. Thorburn AN, Foster PS, Gibson PG, Hansbro PM. Components of Streptococcus pneumoniae suppress allergic airways disease and NKT cells by inducing regulatory T cells. *J Immunol*. 2012;188(9):4611–4620.
61. Essilfie AT, et al. Macrolide therapy suppresses key features of experimental steroid-sensitive and steroid-insensitive asthma. *Thorax*. 2015;70(5):458–467.
62. Plank MW, et al. MicroRNA Expression Is Altered in an Ovalbumin-Induced Asthma Model and Targeting miR-155 with Antagomirs Reveals Cellular Specificity. *PLoS ONE*. 2015;10(12):e0144810.
63. Preston JA, et al. Inhibition of allergic airways disease by immunomodulatory therapy with whole killed Streptococcus pneumoniae. *Vaccine*. 2007;25(48):8154–8162.
64. Asquith KL, et al. Interleukin-13 promotes susceptibility to chlamydial infection of the respiratory and genital tracts. *PLoS Pathog*. 2011;7(5):e1001339.
65. Starkey MR, et al. Constitutive production of IL-13 promotes early-life Chlamydia respiratory infection and allergic airway disease. *Mucosal Immunol*. 2013;6(3):569–579.
66. Starkey MR, et al. Tumor necrosis factor-related apoptosis-inducing ligand translates neonatal respiratory infection into chronic lung disease. *Mucosal Immunol*. 2014;7(3):478–488.
67. Kim RY, et al. MicroRNA-21 drives severe, steroid-insensitive experimental asthma by amplifying phosphoinositide 3-kinase-mediated suppression of histone deacetylase 2. *J Allergy Clin Immunol*. 2017;139(2):519–532.